Journal of Industrial and Engineering Chemistry 21 (2015) 1160–1166

Contents lists available at ScienceDirect

Journal of Industrial and Engineering Chemistry

journal homepage: www.elsevier.com/locate/jiec

New synthetic mercaptoethylamino homopolymer-modified maghemite nanoparticles for effective removal of some heavy metal ions from aqueous solution

Tayyebeh Madrakian *, Abbas Afkhami, Borhan Zadpour, Mazaher Ahmadi

Faculty of Chemistry, Bu-Ali Sina University, Faj av., Hamedan 6517838695, Iran

ARTICLE INFO

Article history:
Received 1 February 2014
Received in revised form 16 May 2014
Accepted 20 May 2014
Available online 27 May 2014

Keywords:
Magnetic nanoparticles
Removal
Heavy metal ions
Polymer

ABSTRACT

A maghemite nanoparticles modified with homopolymers of a new mercaptoethylamino monomer (MAMNPs) have been prepared. The MAMNPs nanoparticles were fully characterized by FT-IR, XRD, BET and TEM measurements. The influences of parameters including pH, dosage of adsorbent and contact time have been investigated in order to find the optimum adsorption conditions. Metal ions adsorption process was thoroughly studied from both kinetic and equilibrium points of view. MAMNPs showed high tendency to investigated metal ions, in this order: Ag(I) > Hg(II) > Pb(II) > Cd(II), owing to the strong contribution of surface loaded polymer.

1. Introduction

The disposal of heavy metal ions in processed water is still a considerable amount [1]. Some metals like lead, arsenic, copper, mercury, antimony, chromium, manganese, and cadmium are significantly toxic to ecological systems and human beings [2–5]. The removal of those harmful metal ions from environment has been a global concern for the last few decades.

So far, various kinds of physical and chemical methods such as ion exchange [6], adsorption [7–10], chemical precipitation [11], reverse osmosis [12] and membrane process [13] have been employed for separation of heavy metal ions from wastewater. Among the available methods, adsorption technology is the most promising and frequently used technique due to its simplicity, high efficiency, and low cost [14,15]. Recently, many research groups have been explored several nanoparticles for removal purposes because of the ease of modifying their surface functionality and their high surface area to volume ratio for increased adsorption capacity and efficiency. In the last decade, magnetic nanoparticle (MNP) adsorption has attracted much interest and is an effective and widely used process because of its simplicity and easy operation [16–19].

In recent years, much attention has focused on surface functionalized MNP such as MNP polymers with core–shell nanostructures, because the polymer shell prevents the core part from particle–particle aggregation and improves the dispersion stability of the core–shell nanostructures in suspension medium [20–25]. For the adsorption of heavy metal ions like Hg^{2+}, Pb^{2+}, Cu^{2+}, Cd^{2+}, and so on, unmodified MNP have a little adsorption capacity [26–28]. At present, there are several routes for surface modification of nanoparticles. For example in order to increase complexation affinity for Hg^{2+}, Thiol-functionalization has been performed [29,30], however, the amino-functionalized are more suitable for Cu^{2+}, Ni^{2+}, Zn^{2+}, and Cd^{2+} ions, [31,32].

In this paper, we report on our preparation and characterization of maghemite nanoparticles (MNPs, γ-Fe_2O_3) modified with a homopolymers of a new mercaptoethylamino monomer (Mercaptoethylamino coated MNPs, MAMNPs). We have investigated the adsorption capacity of MAMNPs for some heavy metal ions (Cd^{2+}, Hg^{2+}, Pb^{2+}, Ag^{+}) in different solution pH and the metal ion uptake capacity as a function of contact time and metal ion concentration. We also studied the adsorption isotherms and kinetics to understand the mechanism of the synthesized MAMNPs metal ions adsorbing and explored desorption and MAMNPs reuse.

* Corresponding author. Tel.: +98 811 8380709; fax: +98 811 8380709.
E-mail addresses: madrakian@basu.ac.ir, madrakian@gmail.com (T. Madrakian).

http://dx.doi.org/10.1016/j.jiec.2014.05.029
1226-086X/

2. Experimental

2.1. Reagents and apparatus

We used a Metrohm model 713 (Herisau, Switzerland) pH-meter for pH measurement. The concentration of metal ions was determined by flame atomic absorption spectrometry using an Aurora model Spect AI 1200 apparatus. The instrumental settings of the manufacturer were followed. Transmission electron microscopy (TEM) involved use of TEM, Philips, CM10, 100 KV transmission electron microscope. X-ray diffraction (XRD) measurement involved use of an X-ray diffractometer (XRD) (38066 Riva, d/G.Via M. Misone, 11/D (TN) Italy) at ambient temperature with Copper *K*-alpha (Cu *K*α) radiation. Infra-red (IR) spectra were recorded with use of a Fourier transform infrared spectrometer (FT-IR, Perkin Elmer, spectrum 100). Specific surface area and porosity were defined by N_2 adsorption–desorption porosimetry (77 K) using a porosimeter (Bel Japan, Inc.).

All the chemicals used were of analytical reagent grade or the highest purity available and were purchased from Merck Company (Darmstadt, Germany). Aqueous solutions of chemicals were prepared with double distilled water (DDW). Standard solutions of Pb(II), Cd(II), Hg(II) and Ag(I) ions were prepared from the nitrate salts of these ions each as 1000 mg L^{-1}. Working solutions, as per the experimental requirements, were freshly prepared from the stock solution for each experimental run. The adjustments of pH were performed with 0.01–1.0 mol L^{-1} HCl and NaOH solutions.

2.2. Preparation of maghemite nanoparticles (MNPs)

MNPs were prepared according to the previously reported procedure [33].

2.3. Preparation of mercaptoethylamino monomer and mercaptoethylamino homopolymer coated MNPs (MAMNPs)

The mercaptoethylamino monomer was synthesized according to a previously reported procedure with some modifications [24]. Briefly, the mercaptoethylamino monomer was synthesized by slow addition of 1 g (0.01 mol) maleic anhydride to the solution of 1.7 g (0.015 mol) cysteamine hydrochloride in 20 mL DDW. The solution was heated at 120 °C for 1 h, until all the water was removed and cysteamine reacted with maleic anhydride through ring opening (Scheme 1). In order to prepare MAMNPs, the mercaptoethylamino monomer was polymerized in the presence of MNPs (0.5 g) and ammonium persulfate (0.1 g, as the initiator) in 30 mL DDW at 85 °C for 12 h. The product was separated by a magnet and washed with methanol to remove unreacted reagents and then DDW. And, the resulting MAMNPs nanoparticles were dried under vacuum for 12 h.

2.4. Adsorption measurement

Adsorption of metal ions from aqueous solution was measured in batch experiments. We studied the effect of pH (3.0–9.0), kinetics time (0–120 min), and adsorption isotherms of metal ions (Cd^{2+}, Hg^{2+}, Pb^{2+} and Ag^{+}). Analyzing adsorption behavior of the MAMNPs involved adding 0.03 g of MAMNPs to 20.0 mL of solution of the metal ions at concentrations of 20 mg L^{-1} at 298 K. The initial pH adjusted using 0.01–1.0 mol L^{-1} HCl and NaOH solutions. The quasi-equilibrium time was 100 min, when the adsorption behavior reached equilibrium. The adsorbents were separated by powerful magnets.

2.5. Desorption experiment

To evaluate the ability to reuse the MAMNPs nanoparticles, we investigated the effects of various desorption solvents on the stability of the adsorbents and the adsorption efficiency of metal ions. Desorption experiments involved adding 0.03 g metal ion-loaded adsorbents to 4.0 mL of desorbing solvent. The mixture was shaken for 20–25 min to reach desorption equilibrium.

2.6. Point of zero charge of the adsorbent (pH_{pzc})

The point of zero charge (pzc) is a characteristic of metal oxides (hydroxides) and of fundamental importance in surface science. It is a concept relating to the phenomenon of adsorption and describes the condition when the electrical charge density on a surface is zero. The surface charge of MAMNPs with carboxylic acid and amino groups is largely dependent on the pH of the solution, the pH_{pzc} caused by the amphoteric behavior of hydroxylated surface groups, and the interaction between surface sites and the electrolyte species. When brought into contact with aqueous solutions, hydroxyl groups of surface sites can undergo protonation or deprotonation, depending on the solution pH, to form charged surface species. In this study, the pH_{pzc} of the MAMNPs was determined in degassed 0.01 mol L^{-1} $NaNO_3$ solution at 20 °C.

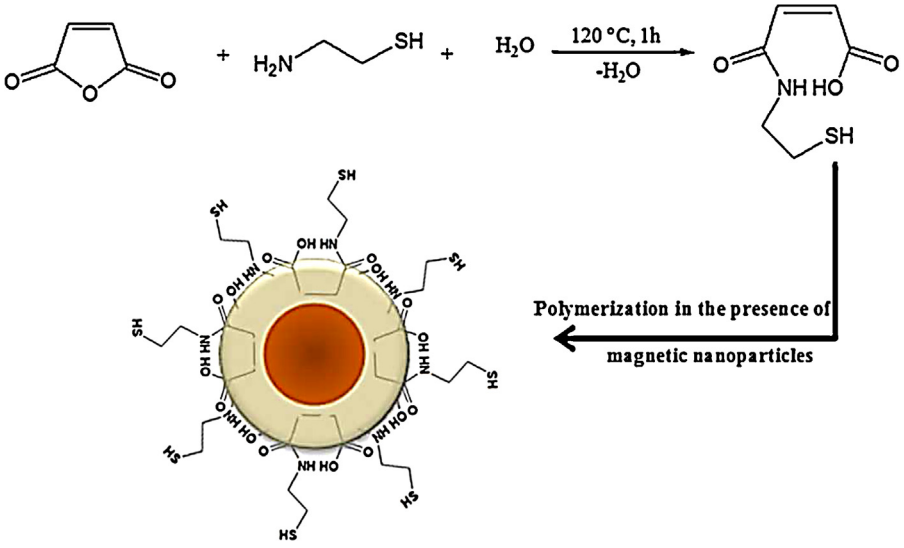

Scheme 1. Schematic representations of MAMNPs nanoparticles synthesis.

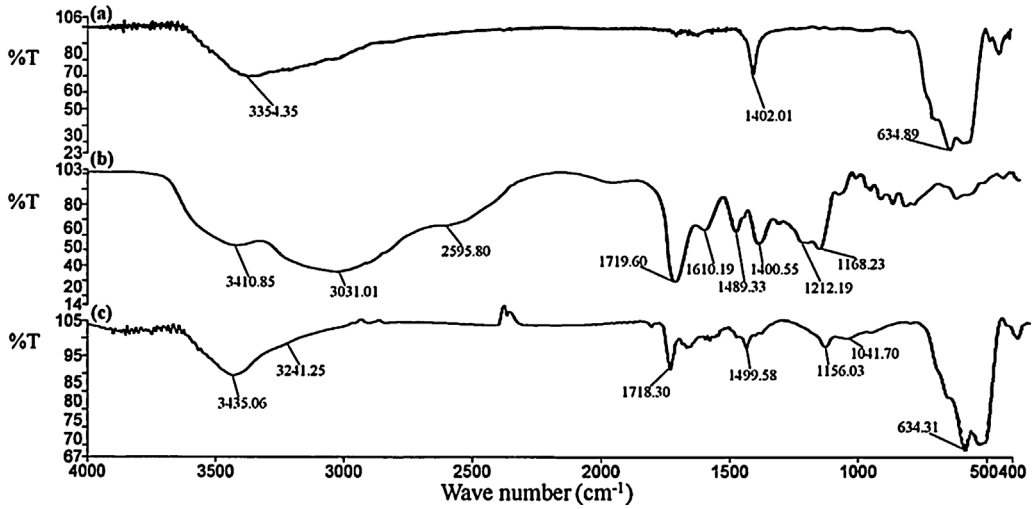

Fig. 1. FT-IR spectra of (a) MNPs, (b) Mercaptoethylamino monomer and (c) MAMNPs.

Aliquots of 30 mL 0.01 mol L^{-1} $NaNO_3$ were mixed with 30 mg MAMNPs in several beakers. pH of the solutions were adjusted at a range of 3.0–10.0 using 0.01 mol L^{-1} of HNO_3 and/or NaOH solutions as appropriate. The initial pHs of the solutions were recorded, and the beakers were covered with parafilm and shaken for 24 h. The final pH values were recorded and the ΔpH (the differences between the initial and the final pH) of the solutions were plotted against their initial pH values. The pH_{pzc} for MAMNPs was determined using the above procedure and was obtained as almost 4.6 where ΔpH = 0 [24].

3. Results and discussion

3.1. Characterization of the adsorbents

The FTIR spectra of the products in each step of the MAMNPs synthesis were recorded to verify the formation of the expected products. The related spectra are shown in Fig. 1. The characteristic absorption band of Fe–O in MNPs (around 634 cm^{-1}) was observed in Fig. 1a. In Fig. 1b the bands around 1168, 1610, 1719, 2595 and 3031 cm^{-1} observed in synthesized monomer can be attributed to the presence of C–N, C=C, C=O, S–H, and =CH groups, respectively. Two new absorption peaks at 1718 cm^{-1} and 1156 cm^{-1} in Fig. 1c are assigned to C=O and C–N bands in the polymer-coated final product (MAMNPs). Moreover, a new absorption peak at 3241 cm^{-1} is related to the stretching modes of the amino group (N–H) [3,34]. Based on the above results, it can be concluded that the fabrication procedure (Section 2.3) has been successfully performed.

The XRD pattern (Fig. 2) shows diffraction peaks that are indexed to (2 2 0), (3 1 1), (4 0 0), (4 2 2), (5 1 1) and (4 4 0) reflection characteristics of the cubic spinel phase of maghemite (JCPDS powder diffraction data file no. 39-1346), revealing that the resultant nanoparticles are mostly γ-Fe_2O_3. The crystallite size was obtained around 11.3 nm from the XRD pattern according to Scherrer equation [33].

TEM image revealed that the diameters of the MNPs as typically 15–25 nm (Fig. 3a), with a generally homogeneous size. The immobilization of the homopolymer in the edges could be observed in Fig. 3b.

Specific surface areas are commonly reported as BET surface areas obtained by applying the theory of Brunauer, Emmett, and

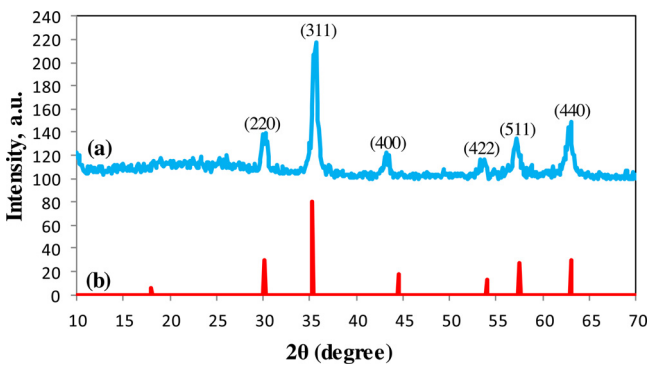

Fig. 2. (a) XRD patterns of the MAMNPs nanoparticles and (b) JCPDS card NO. 39-1346.

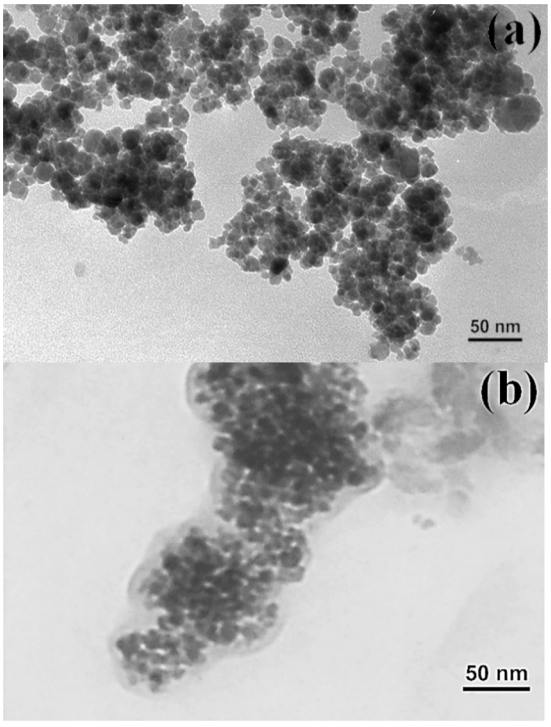

Fig. 3. Transmission electron microscopy of magnetic nanoparticles. (a) MNPs and (b) MAMNPs.

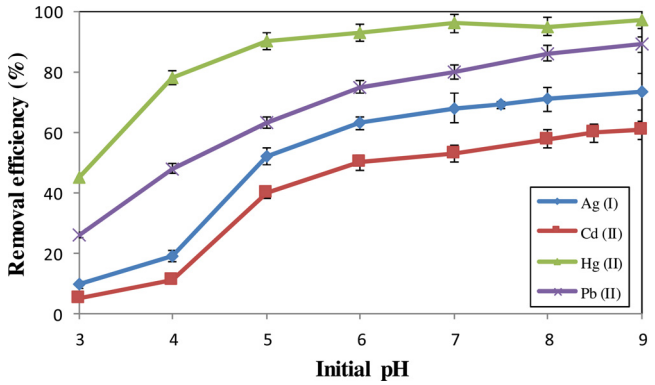

Fig. 4. Effect of pH on the adsorption of metal ions; adsorbent: 0.01 g, initial concentration of metal ions: 20.0 mg L^{-1}, volume of metal ions solution: 20.0 mL, time: 60 min, at 298 K.

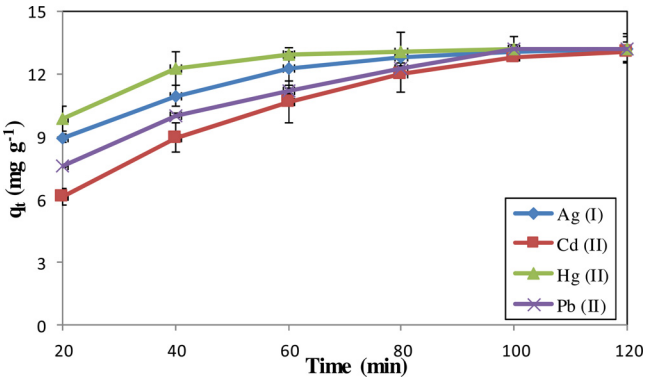

Fig. 5. Effect of time on the adsorption of metal ions; adsorbent: 0.03 g, initial concentration of metal ions: 20.0 mg L^{-1}, volume of solution: 20.0 mL, pH: 6.0, at 298 K.

Teller (BET) to nitrogen adsorption/desorption isotherms measured at 77 K. The specific surface area of the sample is determined by physical adsorption of a gas on the surface of the solid and by measuring the amount of adsorbed gas corresponding to a monomolecular layer on the surface. The data are treated according to the BET theory [35]. The specific surface area of MAMNPs nanoparticles, obtained by BET analysis, was 92.41 $m^2\ g^{-1}$, and the mean pore diameter was 12.23 nm, with a total pore volume of 0.2831 $cm^3\ g^{-1}$.

3.2. Adsorption properties of the MAMNPs for metal ions

The effect of initial solution pH on removal efficiencies is shown in Fig. 4 and indicated that the removal efficiency increased with increasing pH from 3.0 to 5.0, but changed little at pH > 5.0.

The observed dependence of adsorption on pH maybe attributed to change in the surface of the adsorbents with change in pH, which was consistent with the pH-dependent zeta-potential of MAMNPs. The pH of zero point charge (pH_{pzc}) was 4.6. At low pHs ($pH < pH_{pzc}$), the surface of the adsorbents presents in positive (or neutral) form and has less adsorption. As the alkalinity of solution increases, the carboxylic acid functional groups turn into carboxylate anions and the adsorption increases gradually until $pH > pH_{pzc}$. After then, carboxylic acid functional groups completely turn into carboxylate anions, with almost no change in adsorption. Considering that the metal ions might precipitate as hydroxide we chose pH 6.0 for further experiments. The probable adsorption mechanism is shown in Scheme 2. The metal ions mainly interacted with the adsorbents by chelation between the ions and the carboxylate and thiolate anions [36].

Furthermore we studied the dependence of the adsorption of cations on the amount of modified nanoparticles at room temperature and at pH 6.0 by varying the adsorbent amount from 0.01 to 0.09 g in contact with 20.0 mL solution of the mixture of 20 mg L^{-1} each of cations. The suspension was then stirred for 60 min. After magnetically filtering, the supernatant was analyzed for the remaining cations. The results showed that the percentage removal of cations increased by increasing the amount of adsorbent due to the greater availability of the adsorbent. The adsorption reached a maximum with 0.03 g of adsorbent for all investigated metal ions. And the maximum percentage removal was about 98%.

Fig. 5 shows the effects of contact time on the adsorption of the metal ions. The metal ions reached equilibrium at about 100.0 min. In fact, 95% of the metal ions were adsorbed at about 80.0 min. To ensure the equilibrium, we used shaking for 100.0 min for all further experiments. The adsorption kinetics of metal ions with MAMNPs was investigated by pseudo-first order and pseudo-second order kinetic models, for Eqs. (1) and (2), respectively [37,38].

Pseudo-first order model:

$$\ln(q_e - q_t) = \ln q_e - k_1 t \tag{1}$$

Pseudo-second order model:

$$\frac{t}{q_t} = \frac{1}{k_2 q_e^2} + \frac{1}{q_e} t \tag{2}$$

where q_t (mg g^{-1}) is the adsorption capacity at time t (min); q_e (mg g^{-1}) is the adsorption capacity at adsorption equilibrium; and k_1 (min^{-1}) and k_2 (g $mg^{-1}\ min^{-1}$) are the kinetic rate constants for the pseudo-first order and the pseudo-second order models, respectively. The kinetic adsorption data were fitted to Eqs. (1) and (2), and the calculated results are shown in Table 1. The correlation coefficients (R^2) for the pseudo-second order adsorption model were all higher than the correlations for the pseudo-first order model. Therefore, the adsorption data are well represented by the pseudo-second order kinetic model.

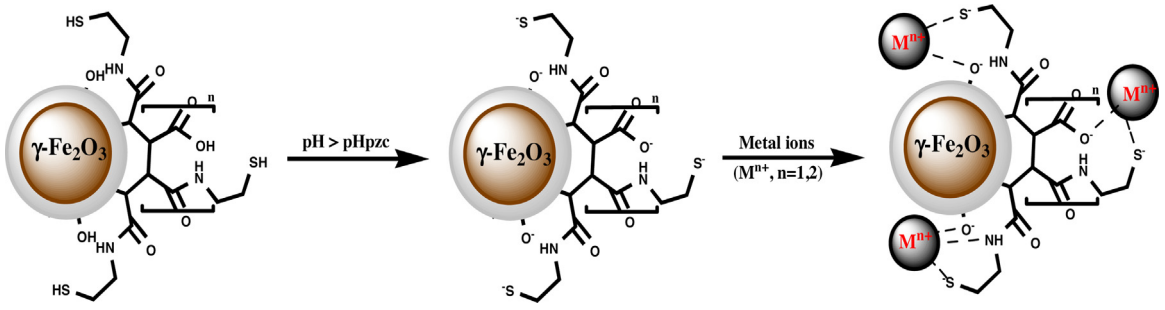

Scheme 2. Schematic representations of possible mechanism for adsorption of metal ions by MAMNPs.

Table 1
The values of parameters obtained by different kinetic models.

Metal ions	Pseudo-first order			Pseudo-second order			R^2
	$q_{e,exp}$ (mg g^{-1})	$q_{e,cal}$ (mg g^{-1})	k_1 (min^{-1})	R^2	$q_{e,cal}$ (mg g^{-1})	k_2 (g mg^{-1} min^{-1})	
Pb(II)	12.28	12.11	0.162	0.997	12.36	0.044	0.999
Hg(II)	24.96	24.44	0.074	0.989	24.67	0.004	0.997
Cd(II)	11.92	10.87	0.061	0.969	12.04	0.008	0.990
Ag(I)	16.21	17.98	0.046	0.990	16.86	0.004	0.996

This result was expected because the usual exchange processes are more rapid and are controlled mainly by diffusion, whereas those with a chelating exchanger are slower and are controlled by a second-order chemical reaction. In addition, MAMNPs, which has chelating functional groups on its surface, most probably behaves as a chelating exchanger. Therefore, the complexation chemical reaction is expected in the adsorption processes [39]. And the rate-limiting step of the adsorption was dominated by a chemical adsorption process [40].

The equilibrium data were analyzed in accordance with the Langmuir, Freundlich, Redlich–Peterson, Sips and Temkin isotherm models.

The linear form of the Langmuir isotherm is (Eq. (3)) [41]:

$$\frac{C_e}{q_e} = \frac{1}{K_L q_m} + \frac{1}{q_m} C_e \tag{3}$$

where K_L is a constant and C_e is the equilibrium concentration (mg L^{-1}), q_e is the amount of metal ion adsorbed per gram of adsorbent (mg g^{-1}) at equilibrium concentration C_e, and q_m is the maximum amount of solute adsorbed per gram of surface (mg g^{-1}), which depends on the number of adsorption sites. The Langmuir isotherm shows that the amount of solute adsorption increases as the concentration increases up to a saturation point.

The linear form of Freundlich empirical model is represented by (Eq. (4)) [42]:

$$\ln q_e = \ln k_f + \frac{1}{n} C_e \tag{4}$$

where K_f (mg$^{1-1/n}$ L$^{1/n}$ g^{-1}) and $1/n$ are Freundlich constants depending on the temperature and the given adsorbent–adsorbate couple. The parameter n is related to the adsorption energy distribution, and K_f indicates the adsorption capacity.

The Redlich–Peterson [43] isotherm is an empirical isotherm incorporating three parameters. It combines elements from both the Langmuir and Freundlich equations, and the mechanism of adsorption is a hybrid and does not follow ideal monolayer adsorption (Eq. (5)):

$$q_e = \frac{K_R C_e}{1 + \alpha_R C_e^{\beta}} \tag{5}$$

where K_R is the Redlich–Peterson isotherm constant (L g^{-1}), α_R is also a constant having unit of (mg^{-1}) and β is an exponent that lies between 0 and 1.

Sips isotherm [44] is a combined form of Langmuir and Freundlich expressions deduced for predicting the heterogeneous adsorption systems and circumventing the limitation of the rising adsorbate concentration associated with Freundlich isotherm model. At low adsorbate concentrations, it reduces to Freundlich isotherm; while at high concentrations, it predicts a monolayer adsorption capacity characteristic of the Langmuir isotherm (Eq. (6)):

$$q_e = \frac{q_m K_S C_e^{1/n}}{1 + K_S C_e^{1/n}} \tag{6}$$

where q_m is the Sips maximum adsorption capacity (mg g^{-1}), K_S the Sips equilibrium constant (L mg^{-1}), and $1/n$ is the Sips model exponent.

The derivation of the Temkin isotherm assumes that the fall in the heat of adsorption is linear rather than logarithmic, as implied in the Freundlich equation. The linear form of Temkin isotherm is (Eq. (7)) [45]:

$$q_e = \frac{RT}{b} \ln K_T + \frac{RT}{b} \ln C_e \tag{7}$$

where K_T is the equilibrium binding constant, corresponding to the maximum binding energy, and constant b is related to the heat of adsorption.

After the equilibrium adsorption data were fitted with different isotherm models with nonlinear or linear regression, the fitting parameter values are summarized in Table 2.

Table 2
Adsorption isotherm parameters for various two and three parameters adsorption isotherm models for the adsorption of investigated cations onto MAMNPs at 25 °C.

Isotherm models	Parameters	Metal ions			
		Pb(II)	Hg(II)	Ag(I)	Cd(II)
Langmuir	K_L (L g^{-1})	0.260	0.028	0.117	0.144
	q_m(mg g^{-1})	130.12	237.46	218.42	91.46
	R^2	0.850	0.950	0.974	0.994
Freundlich	K_f (mg$^{1-1/n}$ L$^{1/n}$ g^{-1})	31.47	32.25	57.88	22.98
	$1/n$	0.31	0.35	0.28	0.30
	R^2	0.810	0.959	0.956	0.954
Redilch–Peterson	K_R (L g^{-1})	28.106	32.012	33.370	14.099
	α_R	0.0840	0.2411	0.2182	0.1741
	β	1.21	0.93	0.92	0.97
	R^2	0.910	0.974	0.985	0.994
Sips	q_m (mg g^{-1})	118.51	237.60	260.55	91.55
	$1/n$	1.21	0.74	0.65	0.99
	K_s	0.003	0.028	0.176	0.144
	R^2	0.976	0.981	0.990	0.999
Temkin	B (J mol^{-1})	58.31	60.96	72.21	54.36
	K_{Te} (L g^{-1})	1.29	3.01	2.23	1.21
	R^2	0.857	0.880	0.922	0.982

Table 3
Effect of different eluents on desorption recovery (%).

Eluent	Recovery (%)			
	Pb^{2+}	Cd^{2+}	Hg^{2+}	Ag^{+}
0.05 mol L^{-1} HCl	42.33	33.74	46.12	27.02
0.05 mol L^{-1} HNO_3	72.65	69.21	82.45	65.24
0.05 mol L^{-1} HNO_3 + acetonitrile (1:1, v/v)	98.16	97.34	98.67	97.23

Table 4
Comparison of proposed method with some recent papers.

Type of adsorbent[a]	Adsorption capacity (mg g^{-1})				Reference
	Cd^{2+}	Hg^{2+}	Pb^{2+}	Ag^{+}	
Fe_3O_4@APS@AA-*co*-CA MNPs	29.6	–	166.1	–	[47]
EDCMS	63.3	–	123.0	–	[48]
MMWCN	1.0	–	9.3	–	[49]
SH–Fe_3O_4–NMPs	–	212.8	–	–	[50]
SG–HO–AO	–	154.5	–	–	[51]
CTS	–	526.3	–	–	[52]
Ag–TCM	–	–	–	570.6	[53]
Surface Ag^{+}-imprinted biosorbent	–	–	–	199.2	[54]
Chitosan	–	–	–	33.2	[55]
MAMNPs	91.5	237.6	118.5	260.5	This work

[a] Fe_3O_4@APS@AA-*co*-CA MNPs: Fe_3O_4 nanoparticles modified with 3-aminopropyltriethoxysilane and copolymers of acrylic acid and crotonic acid; EDCMS: chitosan/SiO_2/Fe_3O_4 modified with EDTA; MMWCN: modified multi-walled carbon nanotubes; SH–Fe_3O_4–NMPs: mercapto-functionalize nano magnetic Fe_3O_4 polymers; SG-HO–AO: silica gel supported amidoxime with homogeneous methods; CTS: chitosan functionalized by amino-terminated hyperbranched polyamidoamine polymers; Ag–TCM: thiourea–chitosan coating on the surface of magnetite.

The high value of R^2 infers that the three parameter models best fit the adsorption equilibrium data and the best fitting isotherm model for all metal ions is determined to be Sips isotherm. The maximum adsorption capacity, obtained from Sips model for Ag(I), Hg(II), Pb(II) and Cd(II) are 260.55, 237.60, 118.51 and 91.55 mg g^{-1}, respectively. Adsorption capacity increased in the sequence of Ag(I) > Hg(II) > Pb(II) > Cd(II), where the different adsorption capacity may be due to disparity in cations radius and interaction enthalpy values [46].

3.3. Desorption and repeated use

From the practical point of view, repeated availability is a crucial feature of an advanced adsorbent. For desorption studies, metal adsorbed MAMNPs were first washed by ultrapure water to remove the un-adsorbed metals loosely attached to the vial and adsorbent. In order to estimate the recovery of the metals ion from MAMNPs, desorption experiments with different reagents (0.05 M HCl, 0.05 M HNO_3 and mixture of acetonitrile: 0.05 M HNO_3 (1:1 v/v)) were performed. After adsorption of the metal ions, the adsorbent was magnetically separated. Then 4.0 mL of the eluents was added to the separated adsorbent. Samples were collected after 5, 10, 20 and 30 min contact times with the eluent to evaluate metal recovery by means of a flame atomic absorption spectrophotometer. The results showed that mixture of acetonitrile with 0.05 M HNO_3 is effective as a back-extractant and can be used for the quantitative recovery of the ion metals (Table 3). Desorption rate was found to be rapid as almost 97% desorption completed within 20–25 min for all metal ions. Furthermore the metal ion adsorption capacity of MAMNPs remained almost constant for the 3 cycles, which indicates no irreversible sites on the surface of MAMNPs for desorption with mixture of acetonitrile with 0.05 M HNO_3 and that the reusability of the adsorbents was satisfactory. Our recyclability studies suggest that this nanoadsorbent can be repeatedly used as an efficient adsorbent in water treatment.

4. Conclusion

We have report on the preparation and characterization of MNPs modified homopolymers of a novel mercaptoethylamino monomer (MAMNPs). MAMNPs are excellent for removal of heavy metal ions such as Cd^{2+}, Hg^{2+}, Pb^{2+} and Ag^{+} from aqueous solution and efficiently remove the metal ions with high adsorption capacity at pH 6.0 and could be used as a reusable adsorbent with convenient conditions. In Table 4 we have compared the ability of the proposed adsorbent in removal of Cd^{2+}, Hg^{2+}, Pb^{2+} and Ag^{+} ions from water with some other works [46–54]. This data elucidate strength of MAMNPs in removal of these ions from solutions. In general, the MAMNPs we used had almost higher adsorption capacity than the reported adsorbents and considering reusability, easy synthesis and separation of magnetic nanoparticles, MAMNPs are better adsorbent than others for investigated metal ions.

Acknowledgments

The authors acknowledge the Bu-Ali Sina University Research Council and Center of Excellence in Development of Environmentally Friendly Methods for Chemical Synthesis (CEDEFMCS) for providing support to this work.

References

[1] N.A. Khan, Z. Hasan, S.H. Jhung, J. Hazard. Mater. 244–245 (2013) 444.
[2] C. Liu, Y. Huang, N. Naismith, J. Economy, Environ. Sci. Technol. 37 (2003) 4261.
[3] F. Ke, L.G. Qiu, Y.P. Yuan, F.M. Peng, X. Jiang, A.J. Xie, Y.H. Shen, J.F. Zhu, J. Hazard. Mater. 196 (2011) 36.
[4] T. Madrakian, A. Afkhami, M. Ahmadi, Chemosphere 90 (2013) 542.
[5] G. Itskos, N. Koukouzas, C. Vasilatos, I. Megremi, A. Moutsatsou, J. Hazard. Mater. 183 (2010) 787.
[6] Z.A. AL-Othman, Inamuddin, Mu. Naushad, Chem. Eng. J. 171 (2011) 456.
[7] X.-J. Ju, S.-B. Zhang, M.Y. Zhou, R. Xie, L. Yang, L.-Y. Chu, J. Hazard. Mater. 167 (2009) 114.
[8] M.A. Tofighy, T. Mohammadi, J. Hazard. Mater. 185 (2011) 140.
[9] N. Koukouzas, C. Vasilatos, G. Itskos, I. Mitsis, A. Moutsatsou, J. Hazard. Mater. 173 (2010) 581.

[10] A. Moutsatsou, E. Stamatakis, K. Hatzitzotzia, V. Protonotarios, Fuel 85 (2006) 657.
[11] F.L. Fu, L.P. Xie, B. Tang, Q. Wang, S.X. Jiang, Chem. Eng. J. 189–190 (2012) 283.
[12] A. Afkhami, M. Saber-Tehrani, H. Bagheri, J. Hazard. Mater. 181 (2010) 836.
[13] L.Z. Zhang, Y.-H. Zhao, R.B. Bai, J. Membr. Sci. 379 (2011) 69.
[14] T. Madrakian, A. Afkhami, M. Ahmadi, H. Bagheri, J. Hazard. Mater. 196 (2011) 109.
[15] F. Ge, M.M. Li, H. Ye, B.X. Zhao, J. Hazard. Mater. 211–212 (2012) 366.
[16] S. Huang, D. Chen, J. Hazard. Mater. 163 (2009) 174.
[17] G. Bayramoglu, M. Yakup Arica, J. Hazard. Mater. 144 (2007) 449.
[18] A. Afkhami, M. Saber-Tehrani, H. Bagheri, T. Madrakian, Microchim. Acta 172 (2011) 125.
[19] T. Madrakian, A. Afkhami, M. Ahmadi, Spectrochim. Acta, A 99 (2012) 102.
[20] M.H. Liao, D.H. Chen, Biotechnol. Lett. 24 (2002) 1913.
[21] S.Y. Mak, D.H. Chen, Dyes Pigm. 61 (2004) 93.
[22] Y.C. Chang, D.H. Chen, J. Colloid Interface Sci. 283 (2005) 446.
[23] M.T. Pham, K.K. Soo, J. Nanosci. Nanotechnol. 9 (2009) 905.
[24] T. Madrakian, M. Ahmadi, A. Afkhami, M. Soleimani, Analyst 138 (2013) 4542.
[25] T. Madrakian, A. Afkhami, H. Mahmood-Kashani, M. Ahmadi, Talanta 105 (2013) 255.
[26] C. Huang, B. Hu, Spectrochim. Acta 63 (2008) 437.
[27] M.R. Shishehbore, A. Afkhami, H. Bagheri, Chem. Cent. J. 5 (2011) 41.
[28] J. Hu, G.H. Chen, M.C. Irene, Water Res. 39 (2005) 4528.
[29] B. Chang, X. Sha, J. Guo, Y. Jiao, C. Wang, W. Yang, J. Mater. Chem. 21 (2011) 9239.
[30] G.L. Li, Z.S. Zhao, J.Y. Liu, G.B. Jiang, J. Hazard. Mater. 192 (2011) 277.
[31] X.D. Xin, Q. Wei, J. Yang, L. Yan, R. Feng, G.D. Chen, B. Du, H. Li, Chem. Eng. J. 184 (2012) 132.
[32] M. Machida, B. Fotoohi, Y. Amamo, T. Ohba, H. Kanoh, L. Mercier, J. Hazard. Mater. 221–222 (2012) 220.
[33] T. Madrakian, A. Afkhami, M. Rahimi, M. Ahmadi, M. Soleimani, Talanta 115 (2013) 468.
[34] T. Madrakian, A. Afkhami, M.A. Zolfigol, M. Ahmadi, N. Koukabi, Nano-Micro Lett. 4 (2012) 57.
[35] S. Brunauer, P.H. Emmett, E. Teller, J. Am. Chem. Soc. 60 (1938) 309.
[36] S. Singh, K.C. Barick, D. Bahadur, J. Hazard. Mater. 192 (2011) 1539.
[37] S. Lagergren, Handlingar 24 (1898) 1.
[38] S. Azizian, J. Colloid Interface Sci. 276 (2004) 47.
[39] Y.T. Zhou, B.W. Christopher, H.L. Nie, Colloids Surf., B: Biointerfaces 74 (2009) 244.
[40] Y.F. Lin, H.W. Chen, P.S. Chien, C.S. Chiou, J. Hazard. Mater. 185 (2011) 1124.
[41] I. Langmuir, J. Am. Chem. Soc. 38 (1916) 2221.
[42] H. Freundlich, W. Heller, J. Am. Chem. Soc. 61 (1939) 2228.
[43] O. Redlich, D.L. Peterson, J. Phys. Chem. 63 (1959) 1024.
[44] R. Sips, J. Chem. Phys. 16 (1948) 490.
[45] M.J. Temkin, V. Pyzhev, Acta Physiochim. URSS 12 (1940) 217.
[46] M. Choi, J. Jang, J. Colloid Interface Sci. 325 (2008) 287.
[47] F. Ge, M.-M. Li, H. Ye, B.-X. Zhao, J. Hazard. Mater. 211–212 (2012) 366.
[48] Y. Ren, H.A. Abbood, F. He, H. Peng, K. Huang, Chem. Eng. J. 226 (2013) 300.
[49] S.Z. Mohammadi, D. Afzali, D. Pourtalebi, Cent. Eur. J. Chem. 8 (2010) 662.
[50] S. Pan, Y. Zhang, H. Shen, M. Hu, Chem. Eng. J. 210 (2012) 564.
[51] J. Chen, R.J. Qu, Y. Zhang, C.M. Sun, C.H. Wang, C.N. Ji, P. Yin, H. Chen, Y.h. Niu, Chem. Eng. J. 209 (2012) 235.
[52] F. Ma, R.J. Qu, C.M. Sun, C.H. Wang, C.N. Ji, Y. Zhang, P. Yin, J. Hazard. Mater. 172 (2009) 792.
[53] L. Fan, C. Luo, Z. Lv, F. Lu, H. Qiu, J. Hazard. Mater. 194 (2011) 193.
[54] H. Huo, H. Su, T. Tan, Chem. Eng. J. 150 (2009) 139.
[55] Y. Yi, Y.T. Wang, H. Liu, Carbohdr. Polym. 53 (2003) 425.